

Explosive volcanic eruptions—VII. The ranges of pyroclasts ejected in transient volcanic explosions

S. A. Fagents and L. Wilson

Environmental Science Division, Institute of Environmental and Biological Sciences, Lancaster University, Lancaster LA1 4YQ

Accepted 1992 September 30. Received 1992 September 17; in original form 1992 July 22

SUMMARY

An earlier treatment of the motions of pyroclasts produced in discrete volcanic explosions assumed that clasts were ejected into a stationary atmosphere. We argue here that the air in the vicinity of an explosion site will itself be moving radially away from the source with a speed comparable to that of the clasts, especially at early times after the start of the motion. As a result, the initial relative velocity of clasts and air will be small. In the earlier treatment this relative velocity was inevitably large, leading to an overestimate of the atmospheric drag force at early times and a consequent underestimate of the final clast range. We set up a simple model of the explosion process which allows us to link the initial clast and air velocities and to find an approximation to the subsequent air flow field. Integration of the equations of motion for clasts with a wide range of sizes, densities, initial speeds and initial elevation angles allows the ranges of these clasts to be found. Clast range data from three documented explosive eruptions are re-analysed to yield initial velocities, and the implications of these velocities for pre-explosion pressure conditions are discussed.

Key words: explosion, pyroclast range, volcanic eruptions.

INTRODUCTION

In an earlier paper in this series (Wilson 1972), a computational scheme was described which allowed the trajectories of pyroclasts launched from a chosen point on or above the Earth's surface with a chosen velocity vector to be followed. The calculations took detailed account of aerodynamic drag forces acting on the clasts, and included allowances for the variation of atmospheric properties with height. The scheme was implemented as a series of FORTRAN computer routines and used in two modes (a) to find the fall times of pyroclasts of various sizes and densities from the edges of eruption clouds over a wide range of heights and (b) to predict the ranges of clasts ejected in transient explosive eruptions, with the intention of simulating mainly vulcanian explosions.

The second of these modes gave computed ranges as a function of clast size and density and of the initial speed and elevation angle of the clast. Several authors have used these results to estimate initial velocities of (usually large) clasts ejected in violent explosions, e.g. at Arenal (Wilson 1980), at Sheveluch (Steinberg 1977) and at Ngauruhoe (Nairn 1976). Such initial velocity estimation is valuable because the peak velocity at which clasts are ejected in explosions is

a function of the excess pressure in the expanding volatile phase driving the explosion and of the mass fraction of the exploding gas–rock mixture which consists of volatiles (Wilson 1980). Thus, if clast launch velocities can be deduced from the ranges of the clasts, some constraints can be placed on the combinations of gas pressure and gas content in the source region of the explosion, even if unique values for both parameters cannot be obtained.

The assumptions made by Wilson (1972) in setting up the initial conditions for trajectory calculations were that clasts should be 'launched' from a chosen position and with a chosen speed and elevation into the surrounding atmosphere, which was assumed to be at rest. In reconsidering the factors controlling the dispersal of clasts from various kinds of explosive vent, we have come to realise that this latter assumption is not realistic. Any volcanic explosion which involves the rapid acceleration of a coherent mass of rock, whether from inside a vent or simply by the disruption of a free surface, inevitably involves the displacement *en masse* of the air overlying the accelerated rocks. This displacement is effected by the propagation of a compression wave into the air. In extreme cases, where the rock speed approaches the speed of sound in the air, the compression wave takes the form of a shock, and the

atmospheric consequences (e.g. condensation of water vapour) of the generation of such shocks have been observed in some explosive events (e.g. Nairn 1976). Whatever the amplitude of the pressure wave, continuity requires that the speed of the air in contact with the rock mass be essentially equal to that of the rock, at least initially.

It follows that, as the exploding rock mass disaggregates and makes the transition to a collection of discrete clasts leaving the explosion site, these clasts are initially in contact with air that is travelling at approximately the same speed as the clasts. This is in striking contrast to the assumption made in the earlier work—that the clasts are encountering air that is at rest. In the earlier version, the initial drag force on the clasts, which is proportional to the square of the difference between the clast speed and air speed, was very large, leading to a large initial deceleration. In the scenario treated in this paper, this initial drag force is essentially zero, and drag only becomes important as the speeds of the clasts and the air progressively decouple. It can be anticipated that the launch speed required to enable a clast of a given size and density to reach a given range, especially a large range, will have been overestimated in the earlier treatment, in some cases by a very large factor. We show below that this is indeed the case, and present a re-analysis of three explosive eruptions by way of illustration.

EXPLOSION MODEL

Since we are intending to link the initial velocity of pyroclasts with the initial and subsequent velocity of the air through which they travel, we need a model for the explosion process which controls both velocities. We base this on a model of transient explosive eruptions proposed by Wilson (1980). This model called for a vent geometry such as that in Fig. 1, where there is an essentially cylindrical vent region containing layers of compact rock, exsolved gas and intruded magma. Wilson proposed that after failure of the caprock, it retains its original cross-sectional area with no escape of the expanding gas between the fragmented blocks or at the sides. The author acknowledged that this vent configuration is probably inadequate for explosions where lateral expansion occurs, the model leading to an underestimate of the pressure required to produce a given velocity. Indeed, several accounts of vulcanian eruptions describe significant lateral expansion of the ejected plug of material in the first few seconds of the explosion (e.g. Nairn 1976; Self, Wilson & Nairn 1979).

In this treatment we take partial account of this lateral expansion by employing a more appropriate geometry (Fig. 2). Consider a region subtending a solid angle Ω at a point. Out to a distance r_1 the region is filled with gas at a pressure P_{gz} and density ρ_{gz} . The zone from r_1 to r_2 is solid material with density ρ_s . The gas mass is

$$m_g = (1/3)\Omega r_1^3 \rho_{gz} \quad (1)$$

and the solid mass is

$$m_s = (1/3)\Omega(r_2^3 - r_1^3)\rho_s. \quad (2)$$

The initial gas to solid mass ratio is defined as $n = m_g/m_s$.

After failure of the caprock has occurred, the gas expands

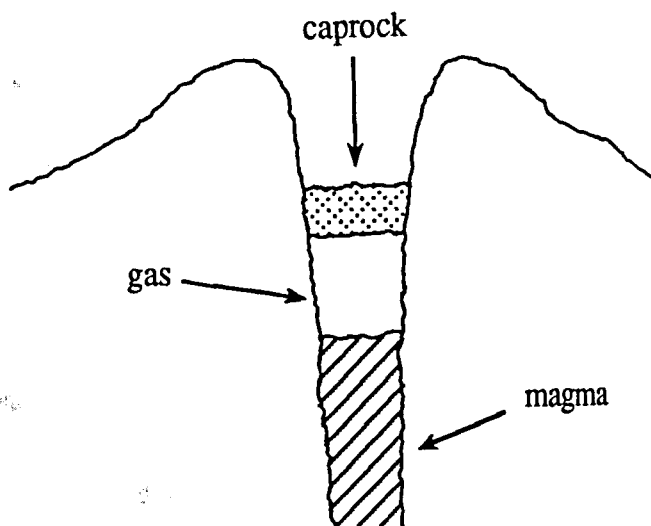


Figure 1. Simplified vent-region geometry for vulcanian eruptions envisaged by Wilson (1980). The vent is considered to be an essentially cylindrical conduit with a gas layer formed above the intruded magma and capped by a layer of compact rock and rubble. At the onset of eruption, the caprock fails and the plug is projected, canon like, vertically into the air, with no allowance for the lateral expansion of the gas/rock mixture.

adiabatically driving the solid material ahead of it. Let $r_{21} = r_2 - r_1$. By the time the inner edge of the solid material has reached a distance r , the mass of air displaced is at least

$$m_a = (1/3)\Omega[(r + r_{21})^3 - r_2^3]\rho_a, \quad (3)$$

where ρ_a is the density of the ambient air.

The equation of motion for the acceleration of the solids plus air is

$$\left[P_{gz} \left(\frac{r_1}{r} \right)^{3\gamma} - P_a \right] \Omega r^2 = \frac{1}{3} \Omega \frac{d^2 r}{dt^2} \{ \rho_s (r_2^3 - r_1^3) + \rho_a [(r + r_{21})^3 - r_2^3] \}$$

i.e.

$$\frac{d^2 r}{dt^2} = \frac{3r^2 [P_{gz} \left(\frac{r_1}{r} \right)^{3\gamma} - P_a]}{\{ \rho_s (r_2^3 - r_1^3) + \rho_a [(r + r_{21})^3 - r_2^3] \}}. \quad (4)$$

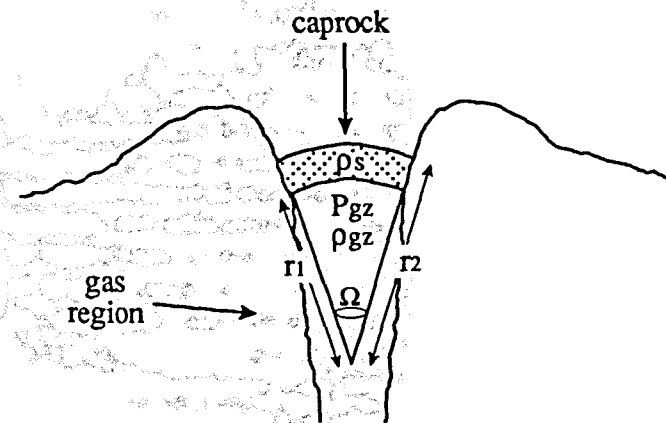


Figure 2. Proposed vent region geometry relevant to our model. Exsolved gas at pressure P_{gz} and of density ρ_{gz} occupies a conical region of radius r_1 which subtends a solid angle Ω hence allowing for varying degrees of lateral expansion above the vent. The gas region is capped by coherent rock of density ρ_s which occupies the region between r_1 and r_2 .

If this equation is integrated twice, the maximum velocity of the expanding envelope, u_0 , can be obtained along with the time t_0 and the distance R_0 at which this occurs. It is assumed that, over the relatively small distances and timescales required for u_0 to be attained, the ejected material behaves as a coherent plug, the detailed motion of the gas attempting to escape between the clasts of the fractured caprock being neglected for the reasons given by Wilson (1980). This approach is lent validity by an account of the 1975 February 19 eruption of Ngauruhoe, New Zealand which describes the '...projection above the crater of a dense slug of highly compressed gas and solid ejecta...' (Nairn 1976), implying the coherence of the ejected material in the earliest moments of the explosion.

Once the ejected slug of rock and gas has reached its maximum velocity, it is proposed that the solid material is 'launched' with this velocity into the moving gas, the velocity of which, u , now decays such that at any radial distance R at time t we have

$$u = u_0 \left(\frac{R_0}{R} \right)^2 e^{-t/\tau}, \quad (5)$$

where the time constant τ is related to the ratio of the initial gas pressure to the atmospheric pressure, by:

$$\tau = \frac{P_{gz}}{P_a} t_0. \quad (6)$$

Fig. 3 shows schematically the basis of the model of the explosion and subsequent air motion. The radial variation of u represents the continuity equation for the displaced air, treated as incompressible. The functional form given for τ represents a very simple approximation which appears to account adequately for the fact that the greater the initial pressure in a given mass of volcanic gas, the greater the final volume (and hence mass) of air forced into motion by the

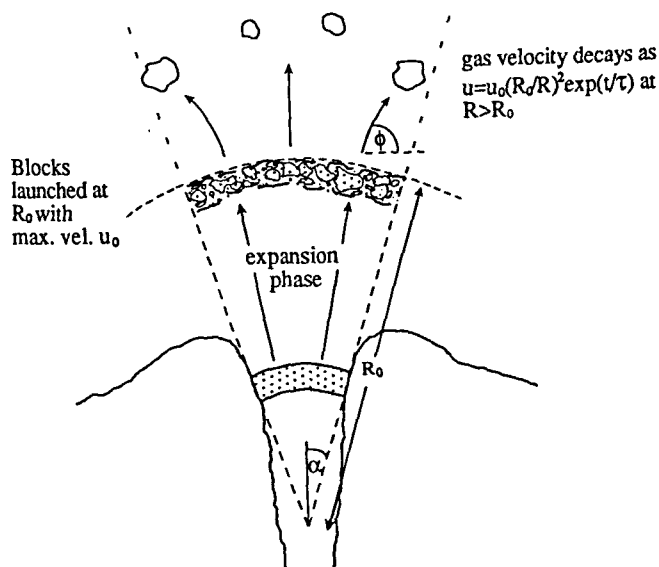


Figure 3. Schematic diagram showing the envisaged initial expansion of the gas/rock mixture out to the distance R_0 where the maximum ejecta velocity u_0 is attained. Blocks of fragmented caprock are then launched with velocity u_0 into the gas flow field, the velocity of which decays as $u = u_0(R_0/R)^2 e^{-t/\tau}$ at distances $R > R_0$.

expansion phase, and the smaller the deceleration of the whole mass in the late stages as the excess pressure decays.

At the point of launch of the fragmented blocks into the gas we employ the computational scheme of Wilson (1972) to simulate the trajectories of the projectiles in the decelerating gas/air mixture. However, at any point on its path a block now experiences a drag force proportional to the square of its velocity relative to the moving air, rather than to the stationary atmosphere as in the earlier treatment.

RESULTS

Eq. (4) was integrated numerically using a FORTRAN computer program to give the velocity and position of ejected material as a function of time, out to the point where the maximum velocity, u_0 , is attained. This was done for a series of explosion sources having wide ranges of values of initial gas pressure, P_{gz} , (0.1 to 100 MPa), gas/solid ratio, n , (0.1 to 30 wt per cent) and initial gas region radius r_1 (1 to 150 m). Fig. 4 shows the variation of the maximum ejecta velocity with initial vent pressure for different values of the gas/rock mass ratio.

The initial parameters required for the above program (P_{gz} , r_1 and n) were varied by trial and error so that a particular set of maximum velocities were produced, viz. 10, 30, 100 and 300 m s^{-1} . These velocities were subsequently passed on to the trajectory computation subroutines, along with the time taken to complete the initial expansion phase, t_0 , and the distance R_0 at which this occurs. The atmospheric gas velocity was caused to vary with position and time in the way described by eqs (5) and (6). Tables 1 to 6 summarize the ranges found for particles with densities between 500 and 3500 kg m^{-3} and radii between 1 mm and 1 m, launched into moving gas with the above velocities.

Tables 1, 2 and 3 show logarithms (to base 10) of ranges (in cm) of particles launched at the end of the expansion phase with elevation angles of $\phi = 45^\circ$, 66° and 87° respectively. These angles are the same as those used by Wilson (1972), and were chosen to provide a reasonable

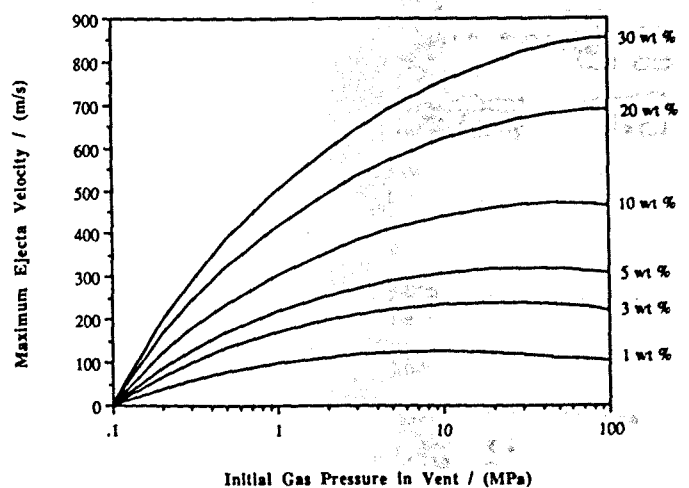


Figure 4. Maximum velocity of ejected material (u_0) as a function of pressure beneath the caprock (P_{gz}). Curves are shown for six values of the weight percentage (n) of ejecta that consists of gas with molecular weight 18, i.e. H_2O .

Table 1. Logarithms (to base 10) of ranges (in centimetres) of particles launched at 45°. Initial gas region radius 25 m, gas to rock mass ratio 0.05.

Velocity / (m s ⁻¹)	Density / (g cm ⁻³)	Radius in centimetres							log ₁₀ (vacuum range in cm)
		0.1	0.3	1.0	3.0	10.0	30.0	100.0	
10	3.5	3.6195		3.5818		3.5753		3.5750	3.5749
	2.5	3.6355		3.5846		3.5754		3.5750	
	1.0	3.6967		3.5987		3.5762		3.5751	
	0.5	3.7573		3.6197		3.5776		3.5753	
30	3.5	3.8781		3.9844		4.0914		4.1001	4.1017
	2.5	3.8838		3.9594		4.0875		4.0995	
	1.0	3.9374		3.8969		4.0685		4.0963	
	0.5	3.9999		3.8795		4.0415		4.0911	
100	3.5	4.1608	4.1631	4.2820	4.6176	4.7577	4.9222	4.9915	5.0264
	2.5	4.1776	4.1509	4.2301	4.5363	4.7015	4.8886	4.9787	
	1.0	4.2493	4.1664	4.1549	4.3156	4.5349	4.7554	4.9199	
	0.5	4.3190	4.2083	4.1612	4.2010	4.4104	4.6171	4.8438	
300	3.5	4.7358	4.6700	4.6763	4.8930	5.1187	5.4357	5.6875	5.9676
	2.5	4.7659	4.6865	4.6631	4.8154	5.0334	5.3540	5.6254	
	1.0	4.8589	4.7496	4.6890	4.6849	4.8303	5.1106	5.4240	
	0.5	4.9366	4.8098	4.7370	4.6773	4.7224	4.9284	5.2505	

Table 2. Logarithms (to base 10) of ranges (in centimetres) of particles launched at 66°. Initial gas region radius 25 m, gas to rock mass ratio 0.05.

Velocity / (m s ⁻¹)	Density / (g cm ⁻³)	Radius in centimetres							log ₁₀ (vacuum range in cm)
		0.1	0.3	1.0	3.0	10.0	30.0	100.0	
10	3.5	3.5896		3.4259		3.3789		3.3766	3.3762
	2.5	3.6229		3.4449		3.3799		3.3767	
	1.0	3.7133		3.5228		3.3856		3.3775	
	0.5	3.7876		3.5903		3.3952		3.3789	
30	3.5	3.8477		3.8420		3.9358		3.9448	3.9464
	2.5	3.8751		3.8246		3.9317		3.9441	
	1.0	3.9625		3.8132		3.9118		3.9408	
	0.5	4.0501		3.8500		3.8833		3.9354	
100	3.5	4.1604	4.0940	4.1317	4.4326	4.6206	4.7779	4.8567	4.8935
	2.5	4.1909	4.1096	4.1007	4.3499	4.5628	4.7412	4.8431	
	1.0	4.2851	4.1743	4.1123	4.1566	4.3861	4.5984	4.7809	
	0.5	4.3634	4.2353	4.1618	4.1069	4.2516	4.4526	4.6998	
300	3.5	4.7684	4.6784	4.6160	4.7061	4.9582	5.2832	5.5558	5.8383
	2.5	4.8037	4.7047	4.6344	4.6414	4.8715	5.1927	5.4900	
	1.0	4.9057	4.7852	4.7064	4.6265	4.6761	4.9344	5.2752	
	0.5	4.9867	4.8553	4.7670	4.6759	4.5997	4.7522	5.0901	

Table 3. Logarithms (to base 10) of ranges (in centimetres) of particles launched at 87°. Initial gas region radius 25 m and gas to rock mass ratio 0.05.

Velocity / (m s ⁻¹)	Density / (g cm ⁻³)	Radius in centimetres							log ₁₀ (vacuum range in cm)
		0.1	0.3	1.0	3.0	10.0	30.0	100.0	
10	3.5	2.3953		2.4474		2.4792		2.4928	2.5012
	2.5	2.3951		2.4366		2.4764		2.4915	
	1.0	3.7177		2.4036		2.4647		2.4902	
	0.5	3.7975		2.3847		2.4562		2.4868	
30	3.5	2.7051		2.9233		3.0643		3.0908	3.0864
	2.5	2.6805		2.8887		3.0524		3.0927	
	1.0	3.9703		2.7847		3.0140		3.1027	
	0.5	4.0513		2.7140		2.9739		3.1211	
100	3.5	2.9227	3.0157	3.2040	3.5839	3.7963	3.9366	4.0074	4.0405
	2.5	4.1938	2.9756	3.1329	3.4955	3.7160	3.9034	3.9952	
	1.0	4.2972	4.1750	2.9825	3.2303	3.5095	3.7778	3.9382	
	0.5	4.3790	4.2440	2.9262	3.0678	3.3520	3.6072	3.8637	
300	3.5	4.7792	4.6794	3.5078	3.8201	4.0945	4.4524	4.7195	4.9854
	2.5	4.8166	4.7097	3.4568	3.7338	3.9947	4.3682	4.6551	
	1.0	4.9219	4.7974	4.7110	3.5123	3.7476	4.0763	4.4454	
	0.5	5.0640	4.8681	4.7811	3.4185	3.6003	3.8721	4.2383	

Table 4. Logarithms (to base 10) of ranges (in centimetres) of particles launched at 45°. Initial gas region radius 25 m, gas to rock mass ratio 0.10.

Velocity / (m s ⁻¹)	Density / (g cm ⁻³)	Radius in centimetres							log ₁₀ (vacuum range in cm)
		0.1	0.3	1.0	3.0	10.0	30.0	100.0	
10	3.5	3.6175		3.5802		3.5737		3.5734	3.5734
	2.5	3.6334		3.5829		3.5739		3.5735	
	1.0	3.6944		3.5969		3.5747		3.5736	
	0.5	3.7550		3.6177		3.5760		3.5738	
30	3.5	3.8723		3.9811		4.0894		4.0982	4.0998
	2.5	3.8777		3.9558		4.8543		4.0976	
	1.0	3.9305		3.8922		4.0662		4.0943	
	0.5	3.9928		3.8738		4.0389		4.0891	
100	3.5	4.1355	4.1432	4.2697	4.6126	4.7540	4.9202	4.9900	5.0252
	2.5	4.1512	4.1288	4.2154	4.5303	4.6972	4.8863	4.9771	
	1.0	4.2212	4.1404	4.1332	4.3050	4.5282	4.7519	4.9179	
	0.5	4.2903	4.1808	4.1359	4.1845	4.4010	4.6125	4.8411	
300	3.5	4.5220	4.4731	4.5383	4.8311	5.0873	5.4215	5.6798	5.9662
	2.5	4.5487	4.4823	4.5010	4.7392	4.9934	5.3363	5.6164	
	1.0	4.6363	4.5338	4.4866	4.5438	4.7592	5.0769	5.4094	
	0.5	4.7119	4.5892	4.5232	4.4920	4.6171	4.8749	5.2272	

sample of ranges up to the maximum range for clasts launched at a given velocity.

For all three sets of results the initial gas region radius is 25 m and the gas/solid ratio 0.05, thought to be reasonable values for this type of eruptive system. These tables are presented in these units so that they can be directly compared and contrasted with Tables 1 to 3 of Wilson (1972). It will be noted that vacuum range values are slightly larger than those given by Wilson (1972). This is a consequence of taking into account the initial expansion phase of the eruption: the distance out to the point where u_0 is attained is included in the range calculation. The ranges calculated by our method are significantly larger than those of Wilson (1972). The differences are most significant for the smaller particle sizes. This arises from the fact that smaller particles will be more influenced by air motion than will the

larger blocks which, by virtue of their greater inertia, are less readily decelerated or accelerated and are capable of achieving a large fraction of their vacuum range.

Tables 4 and 5 show logarithms of ranges of particles launched at $\phi = 45^\circ$ from an explosion with the same value of $r_1 = 25$ m but with initial gas/solid ratios of $n = 0.10$ and 0.20 respectively. Taken along with Table 1 ($n = 0.05$) it can be seen that, for the same combinations of particle radius and density, smaller values of n produce larger ranges. This is explained by noting that, at lower gas/rock ratios, the pressure required for the exploding material to reach a certain maximum velocity is larger than for higher gas/solid ratios. Since the acceleration of the solid ejecta and air is proportional to P_{gr} , the distance and time at which u_0 is reached are both greater. The velocity decay constant, τ , is therefore increased and so the gas-particle relative velocity

Table 5. Logarithms (to base 10) of ranges (in centimetres) of particles launched at 45°. Initial gas region radius 25 m, gas to rock mass ratio 0.20.

Velocity / (m s ⁻¹)	Density / (g cm ⁻³)	Radius in centimetres							log ₁₀ (vacuum range in cm)
		0.1	0.3	1.0	3.0	10.0	30.0	100.0	
10	3.5	3.6161		3.5790		3.5727		3.5724	3.6507
	2.5	3.6320		3.5818		3.5728		3.5724	
	1.0	3.6929		3.5956		3.5736		3.5725	
	0.5	3.7534		3.6163		3.5749		3.5727	
30	3.5	3.8684		3.9789		4.0880		4.0969	4.1238
	2.5	3.8734		3.9533		4.0840		4.0963	
	1.0	3.9258		3.8890		4.0647		4.0930	
	0.5	3.9879		3.8699		4.0371		4.0877	
100	3.5	4.1191	4.1304	4.2620	4.6094	4.7518	4.9189	4.9891	5.0278
	2.5	4.1341	4.1146	4.2061	4.5265	4.6946	4.8849	4.9761	
	1.0	4.2030	4.1235	4.1193	4.2984	4.5240	4.7497	4.9166	
	0.5	4.2716	4.1630	4.1194	4.1739	4.3951	4.6096	4.8394	
300	3.5	4.4376	4.3979	4.4926	4.8118	5.0785	5.4174	5.6776	5.9655
	2.5	4.4625	4.4030	4.4447	4.7153	4.9820	5.3314	5.6138	
	1.0	4.5472	4.4482	4.4087	4.4968	4.7369	5.0674	5.4052	
	0.5	4.6218	4.5013	4.4288	4.4239	4.5828	4.8587	5.2207	
600	3.5	4.8789	4.8054	4.7863	4.9588	5.2099	5.5800	5.9403	6.5662
	2.5	4.9106	4.8250	4.7850	4.8870	5.1140	5.4767	5.8433	
	1.0	5.0063	4.8936	4.8273	4.7959	4.9047	5.1917	5.5650	
	0.5	5.0849	4.9561	4.8803	4.8084	4.8123	4.9970	5.3519	

increases more slowly subsequent to launch which, along with the larger R_0 , ensures that travel distances are larger.

Table 6, for comparison, shows ranges of particles launched at $\phi = 45^\circ$ but with an initial gas region radius of 50 m. Ranges are significantly greater than for a gas region radius of 25 m. This is due to the increased times and distances necessary for u_0 to be attained.

As well as these general differences, there are also interesting departures from the pattern of ranges in Wilson (1972) within each of these new sets of results. Take, for example, Tables 1 to 3. Two major influences on the particle trajectory make themselves apparent. One is the effect of the expanding gas envelope and reduced drag force on the clast, enabling it to travel further. The other comes into effect at distances where the expanding gas velocity becomes insignificant, and where the stationary ambient air leads to a larger drag force and hence greater deceleration of the clast, tending to inhibit its flight. The interplay between the 'helping' gas and the 'hindering' atmosphere can be seen. Wilson's (1972) results show that for any velocity, particle ranges increase with both density and radius: increasing mass means increased inertia and hence resistance to the decelerating forces of the still air. In our results, however, the pattern is more complex. Take Table 1, for example. For small particle sizes the range increases with decreasing density: low mass particles are, to a certain extent, being entrained by the gas. But for larger particles, range decreases with decreasing density: less dense and hence relatively lighter particles are being more readily decelerated at greater distances by the air drag. The exception to this is the case of 100 cm blocks launched at low velocities (10 m s^{-1}). The ranges are sufficiently short that the blocks never escape the influence of the expanding gas stream.

The gas-atmosphere interplay is also manifested in the variation of range with clast radius. For low velocities, smaller (lighter) particles travel furthest, aided by the gas. For higher velocities (i.e. $>30 \text{ m s}^{-1}$ in Table 1), range at first decreases and then increases with increasing radius. Smaller particles are helped by the gas; then an increase in mass produces a resistance to accelerating forces from the expanding gas. Finally the mass becomes sufficiently great to

resist significantly the decelerating forces of the more distal, nearly still air.

On examination of Tables 1 to 6 it will also be noted that for some combinations of velocity, density and radius the predicted ranges exceed the vacuum ranges. This occurs mostly for low launch angles and velocities. This again may be attributed to the effects of the motion of the gas: the vertical drag forces hinder the settling rate of small clasts while the horizontal component of the air motion carries them sideways.

The model presented here does not try to describe the more complex possible behaviour of the atmosphere, such as the presence of wind shear or the formation of a convecting cloud above the vent. So for smaller and less dense projectiles, i.e. those more vulnerable to atmospheric motion, our results give only a rough idea of expected travel distances. Indeed, it is to be anticipated that at least millimetre-sized particles will commonly be incorporated into volcanic convection clouds over the eruption site. However, the major application of this theory is for the prediction of initial conditions in the vent by using travel distances of large ejected blocks, which are demonstrably less affected by the atmosphere.

APPLICATION TO DOCUMENTED EXPLOSIONS

The July 1968 eruption of Arenal Volcano, Costa Rica

Melson (1972) gave a comprehensive description of the renewal, on July 29, 1968, of eruptive activity of Arenal volcano, which had previously been thought to be extinct. The initial explosive phase devastated the surrounding area and caused much loss of life. Fudali & Melson (1972) described a region of secondary craters formed by impacting debris flung from the vent site. This region extended up to 5 km west of the vent, where craters were observed to have dimensions requiring excavation by an impacting projectile having a kinetic energy of $\sim 10^7$ joules. Fudali & Melson showed, through a series of calculations, that blocks 0.8 m in diameter and having a density of 2600 kg m^{-3} must be

Table 6. Logarithms (to base 10) of ranges (in centimetres) of particles launched at 45° . Initial gas region radius 50 m, gas to rock mass ratio 0.05.

Velocity/ (m s^{-1})	Density/ (g cm^{-3})	Radius in centimetres						$\log_{10}(\text{vacuum range in cm})$
		0.1	0.3	1.0	3.0	10.0	30.0	100.0
10	3.5	3.8874		3.8057				3.7849
	2.5	3.9107		3.8162		3.7860		3.7850
	1.0	3.9852		3.8489		3.7865		3.7851
	0.5	4.0518		3.8875		3.7890		3.7854
30	3.5					3.7931		3.7860
	2.5	4.1275		4.1367				4.1969
	1.0	4.1472		4.1249		4.1921		4.1966
	0.5	4.2221		4.1094		4.1900		4.1966
100	3.5	4.2923		4.1288		4.1794		4.1949
	2.5					4.1641		4.1921
	1.0	4.4301	4.3893	4.4344	4.6852	4.8079	4.9516	5.0126
	0.5	4.4551	4.3952	4.4075	4.6164	4.7599	4.9215	5.0014
300	3.5	4.5398	4.4409	4.3974	4.4520	4.6230	4.8021	4.9495
	2.5	4.6142	4.4939	4.4308	4.4018	4.5280	4.6812	4.8825
	1.0	5.0244	4.9446	4.9038	5.0111	5.1877	5.4670	5.7047
	0.5	5.0574	4.9670	4.9127	4.9570	5.1162	5.3960	5.6458
		5.1552	5.0399	4.9686	4.9154	4.9648	5.1828	5.4590
		5.2344	5.1043	5.0258	4.9444	4.9066	5.0337	5.3044

launched from the vent site with a velocity of at least 600 m s^{-1} to produce such craters at such a distance. They derived a corresponding minimum initial vent pressure of 4700 b (470 MPa) using a modified version of the Bernoulli equation $P_{gz} = 1/2 \rho u_0^2$, where ρ is a density in some way representative of the explosion products. However, this equation was criticised by McBirney (1973), Nairn & Self (1978) and Self *et al.* (1979) for the ambiguity in the definition of ρ , and was shown by Wilson (1980) to be completely inappropriate for calculating vent pressures.

Wilson (1972) noted that another flaw in the calculations of Fudali & Melson is the use of a constant drag coefficient which, given that significant variations of velocity and hence Reynolds number occur along the path, cannot be valid. Wilson inferred that a more appropriate kinetic energy for the impacting missile might be $10^{7.5} \text{ J}$, but subsequently confirmed Fudali & Melson's estimates of velocity, despite the more complex assessment of the drag coefficient and the effects of the atmosphere. However, as stated earlier, Wilson's (1972) analysis neglected the effect of the expanding gas envelope. Also, our careful examination of Fudali & Melson's Fig. 5 suggests that an even more accurate value for the kinetic energy of the impacting blocks might be $10^{7.6} \text{ J}$.

Further errors in the estimation of the maximum ejection velocity would arise from the assumption that particles launched at $\phi = 45^\circ$ travel further than those launched at any other angle. This is true for travel through a vacuum, but the presence of a stratified atmosphere ensures that the optimum elevation angle is less than 45° . So if a *minimum* value for the maximum ejection velocity is required, it is necessary to use this optimum angle, which itself will vary with the initial launch conditions and clast characteristics.

It is also unclear whether Fudali & Melson took into account the net change in elevation that a block would undergo in travelling 5 km west from the vent part of the way up the flank of Arenal. This will have a significant effect on the kinetic energy of the impacting missile.

Our computer program was set up with conditions (altitude, atmospheric pressure, density and temperature) appropriate to the location of the Arenal crater. A vent and run repeatedly to find the initial vent conditions (P_{gz} , r_1 , n), elevation angle and projectile dimension required for impact at 5 km west of and 500 m below the vent site with a kinetic energy of $10^{7.6} \text{ J}$. Examination of preliminary results showed the importance of accurate estimation of clast final kinetic energy if it is to be used as a constraint in modelling explosive eruptions: it may significantly affect the required initial velocity and gas concentration as well as the clast radius and launch angle for a specific clast travel distance to be attained.

Fig. 5 shows the combinations of initial gas region radius r_1 , gas mass fraction n , vent pressure P_{gz} and launch velocity u_0 (reached after the initial expansion phase) that satisfy the conditions on clast range and final kinetic energy. For all the curves shown, the diameter of the block is 1.30 m and it must be launched at an angle of $\phi = 39^\circ$. It can be seen that, for smaller gas region radii, larger gas concentrations and hence greater launch velocities are required for the projectile to reach the required distance possessing the required kinetic energy.

What is perhaps most striking about the results is that, compared with the estimate of Fudali & Melson (1972), very low vent pressures are capable of sending the missile to the required range. This is more in line with the expected fracture strengths of rocks (up to the order of a few tens of

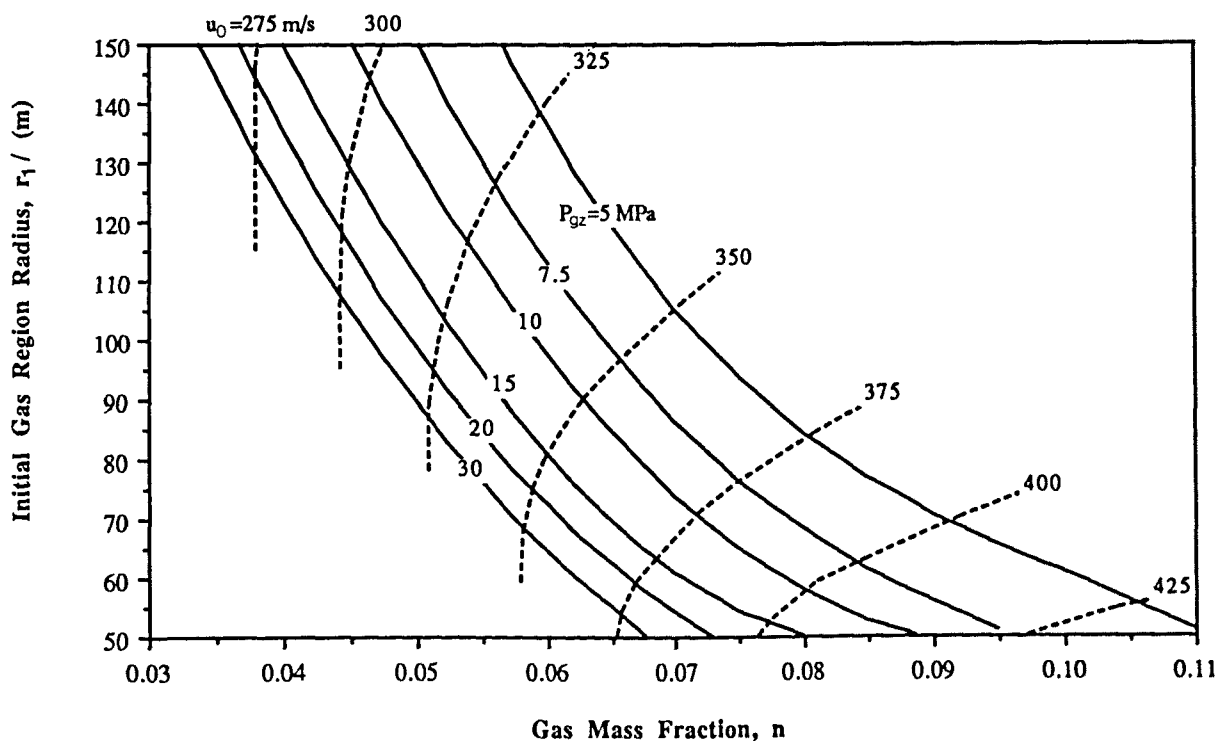


Figure 5. Combinations of initial gas region radius, r_1 , gas/solid mass fraction, n , vent pressure, P_{gz} , and launch velocity, u_0 , that project a 1.30 m diameter block to a distance of 5 km so that it lands with a kinetic energy of $10^{7.6} \text{ J}$. Solid curves show pressures of 5 to 30 MPa, broken curves show velocities of 275 to 425 m s^{-1} .

MPa) based on measurements of tensile and shear strengths of rocks by Roberts (1969) and Murrell (1969).

Uncertainty in defining the initial gas region radius arises from the poorly constrained vent geometry. Fig. 6 of Melson & Saenz (1973) shows the bottom of crater A at Arenal to be approximately $100\text{ m} \times 200\text{ m}$ in size. These dimensions were almost certainly the product of several explosions, with wall failure and slumping likely to have also played a part. However, these dimensions put an upper limit on the gas region radius of around 80 to 140 m if the vent radius is taken as the average (75 m) of the two longest axes of the crater. This range in the gas region radius upper limit is due to the choice of a range of values of Ω , the solid angle subtended by the gas region. A solid angle of 4 steradians corresponds to a gas region radius of 80 m while 1 steradian leads to a radius of 140 m.

In order for this type of eruptive activity to occur, it is expected that there will be significant build up of gas in the vent region, and that it is likely, due to magma interaction with groundwater, that this gas concentration will exceed magmatic gas mass fractions, i.e. $n > 0.03$. This, coupled with the constraint on radius, means that for initial vent pressures of the order 10 MPa, limits on the initial launch velocity might be 300 to 400 m s^{-1} for the Arenal event.

The February 1975 eruption of Ngauruhoe Volcano, New Zealand

The explosions of Ngauruhoe volcano on February 19, 1975 threw out both lithic and juvenile blocks to distances ranging up to approximately 2.8 km from the vent (Nairn 1976). The eruption at 18.10 hr is the best documented and is considered typical of the explosive events. Nairn & Self (1978) described this eruption in detail.

From photographic records of the first few seconds of the eruption, Nairn (1976) estimated the average ejecta slug velocity over the first 300 m above the vent to be in the range 300 to 600 m s^{-1} . By assuming a horizontal range of 2.5 km for a block of diameter 0.8 m and having density 2500 kg m^{-3} , he interpolated a minimum initial velocity of 400 m s^{-1} from the tables of Wilson (1972). Nairn then confirmed that this was of the right order using 1-D shock-tube theory, arriving at a minimum velocity of 340 m s^{-1} . A corresponding explosion pressure of 200 MPa was calculated from McBirney's (1973) equation $P = 0.0125 v^2$, where v is the ejecta velocity (taken as 400 m s^{-1}). It was postulated that such high pressures were the result of rapid heating of meteoric water to magmatic temperatures. However, the constant in the above equation for the pressure suffers from the same criticisms (Wilson 1980) as the density in the modified Bernoulli equation used by Fudali & Melson (1972) for Arenal.

By treating the initial expansion of the ejected material as isothermal, Self *et al.* (1979) calculated that a velocity of 400 m s^{-1} is attainable in the Ngauruhoe explosion with an initial driving pressure of less than 30 MPa. This corresponds to magma water contents of 4 to 10 wt per cent which, as this exceeds typical andesitic magma juvenile water contents, implies that some groundwater was also involved. Wilson (1980) suggested treating the expansion of gas in discrete explosions as adiabatic, but reported that velocities

as high as 400 m s^{-1} can only be reached if high pressures (which are unlikely to be supported by typical rock strengths) and/or large water contents are involved. He suggested that such high velocities deduced from block ranges may well be overestimates arising from errors in the treatment of drag forces on the projectile. This is born out by the current modelling where much lower velocities are inferred.

From the geometry of the vent region of Ngauruhoe (Fig. 6), the minimum launch angle for the blocks of ejecta is around $\phi = 50^\circ$, if it is assumed that the gas/solid mixture expands out of the conduit to fill the crater region. Photographic evidence suggests that this is so (Nairn 1976; Nairn & Self 1978). If this angle is extrapolated back into the vent region a gas region radius of 15 to 38 m is deduced depending on the vent diameter, which cannot be greater than that of the crater bottom (50 m). We have used this geometry in our calculations, but acknowledge that it is not straightforward to apply our model to a situation like that at Ngauruhoe, where repeated explosions involving about 50 per cent non-juvenile material took place from a vent in a crater at the top of a cone. To provide the total volume of non-juvenile clasts erupted during the explosion analysed here and for others on the same day ($\sim 2.5 \times 10^5\text{ m}^3$), Self *et al.* (1979) calculated that the conduit feeding the vent must have had its radius enlarged by an amount of order 20 m over a 500 m vertical extent. We can justify our geometry only if we assume that, each time new magma intrudes the cone, it accumulates the required volume of fragmental rock from the conduit walls and pushes this material ahead of the main part of the melt as it rises. In practice, it is unlikely that the geometry will be quite so simple.

Fig. 7 presents the results of modelling the eruption of a 0.40 m diameter block which is launched at 50° and travels a distance of 2.5 km horizontally, landing at an elevation 980 m below the vent (Nairn 1976). It can be seen that, for pressures ranging up to 10 MPa, gas concentrations of 2 to 6 wt per cent are implied. It is likely that the vent pressure will be in the lower end of the range of pressures displayed in Fig. 7 because there had already been several explosions before the 18.10 hr eruption: the material comprising the

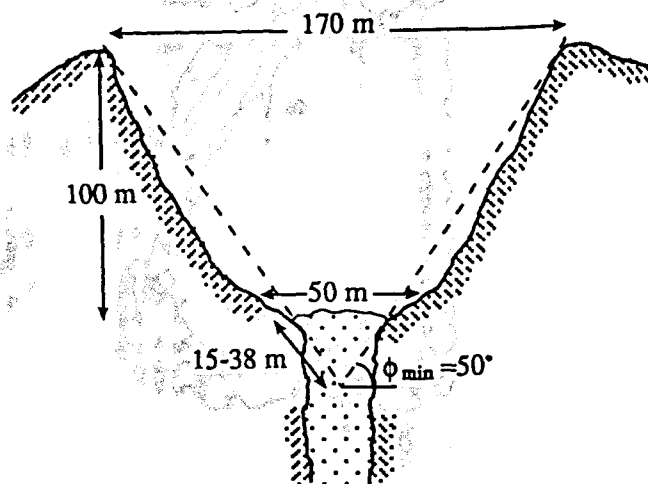


Figure 6. Geometry of the vent region of Ngauruhoe volcano inferred by Self *et al.* (1979). Crater dimensions are well constrained and did not change significantly during the eruption. Diagram not to scale.

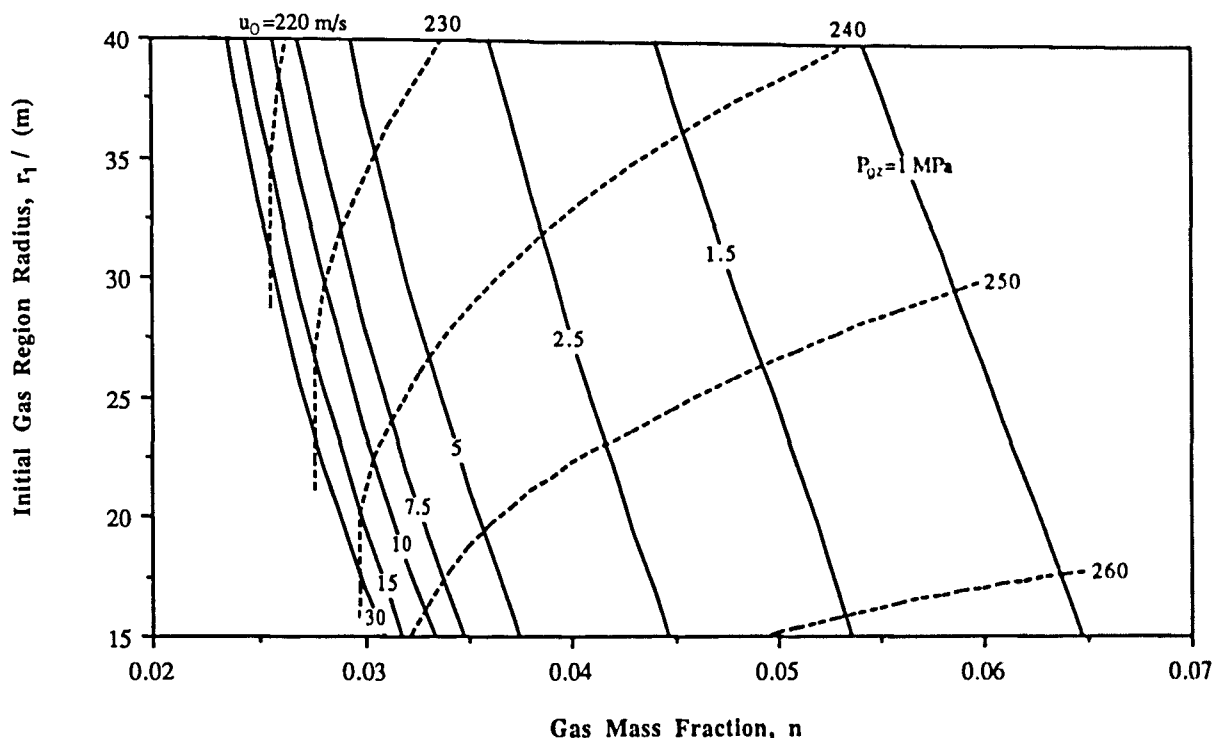


Figure 7. Combinations of r_1 , n , P_{02} and u_0 that project a block 0.80 m in diameter to a distance of 2.5 km from the summit vent of Ngauruhoe. Solid curves represent pressures of 1 to 30 MPa, dashed curves indicate launch velocities of 220 to 260 m s^{-1} .

plug is likely to have been fractured, rubbly rock with possibly a warm juvenile component. The strength of this caprock will therefore be relatively low, and from Fig. 7 this corresponds to the higher end of the range of gas concentrations given. The associated ejecta velocities are in the range 220 to 260 m s^{-1} . This is somewhat lower than the velocity deduced by Nairn (1976) from photographic evidence but, given the uncertainty in the timing of the photographs, it seems that this new velocity estimate is not unreasonable.

The March 1977 eruption of the Ukinrek Maars, Alaska

The chronology, petrology, and dynamics of the Ukinrek maar-forming eruptions are described by Kienle *et al.* (1980) and Self, Kienle & Huot (1980). These explosions occurred over a period of ten days in 1977, when rising basaltic magma met a perched aquifer in the overlying glacial till. Fig. 8 shows the general setting of the Ukinrek Maars.

Examination of the deposits revealed that there were two mechanisms involved in the formation of the larger East Maar (Self *et al.* 1980). Initially, large (2–3 m) lithic blocks were ejected to distances of up to 700 m by the crater-forming phreatomagmatic explosion. These blocks increase in size with distance from the crater and were assumed to be the product of a transient, vulcanian-type explosion. There were termed Type 2 blocks by Self *et al.* Subsequent ejection of both lithic and juvenile material is assumed to have been into a continuous gas-stream, producing a sustained eruption column and a deposit whose block size decreases away from its source. Since it is only the Type 2 blocks that appear to be the product of a transient explosion, it is with those that we are concerned here.

Kienle *et al.* (1980) reported that the first observation of the newly formed crater was made some 6 1/2 hr after the observation of the ash plume which was inferred to have been produced by the maar-forming explosion. The crater diameter at this time was 60 m, which yields an upper limit on the initial gas region radius of ~30 to 55 m if the solid angle Ω is taken to be in the range 1 to 4 steradians. The explosion spread angle, α , (See Fig. 3) is thus in the range 33 to 69° since $\alpha = \cos^{-1}(1 - \Omega/2\pi)$, which consequently constrains the possible clast launch angles.

Our computer program was supplied with the relevant atmospheric and physical characteristics and then run to find the combinations of parameters required to send a 2 m diameter block to a distance of 700 m. The optimum launch angle, ϕ , was found to be ~42°, which requires a solid angle of at least 2 steradians. Fig. 9 presents the results. It can be seen that very low vent pressures and volatile concentrations are necessary for such a distance to be attained. This is consistent with Self *et al.* (1980)'s report that the till in which these craters were formed is expected to have a strength of only a few bars (a few tenths of a MPa). The required gas/solid fraction, despite being small compared with that inferred above from the results for Arenal and Ngauruhoe (Fig. 5, Fig. 7), still represents a significant concentration in the vent. This is because the magma involved in this event, described as '...weakly undersaturated alkali olivine basalt...' (Kienle *et al.* 1980), would typically have volatile contents in the range 0.1 to 1 wt per cent (Basaltic Volcanism Study Project 1981). The reasonably good constraints on gas region radius and vent pressure lead to an inferred gas concentration of 1 to 5 wt per cent, which is consistent with the expected build up of gas that would occur on interaction of the rising magma with the perched aquifer. The velocity

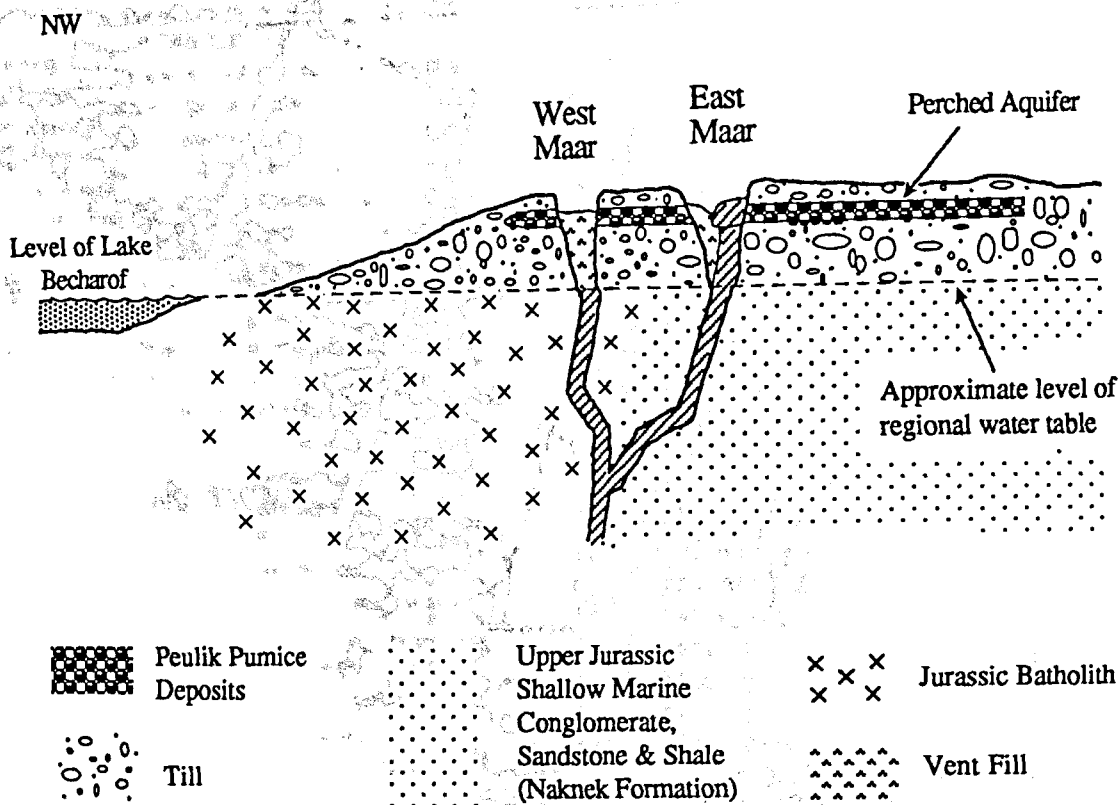


Figure 8. Schematic drawing of the setting of the Ukinrek Maars. The rising magma may have encountered a significant amount of water in the bedrock as well as in the Peulik pumice deposits enclosed within the glacial till. Diagram not to scale. (After Self *et al.* 1980.)

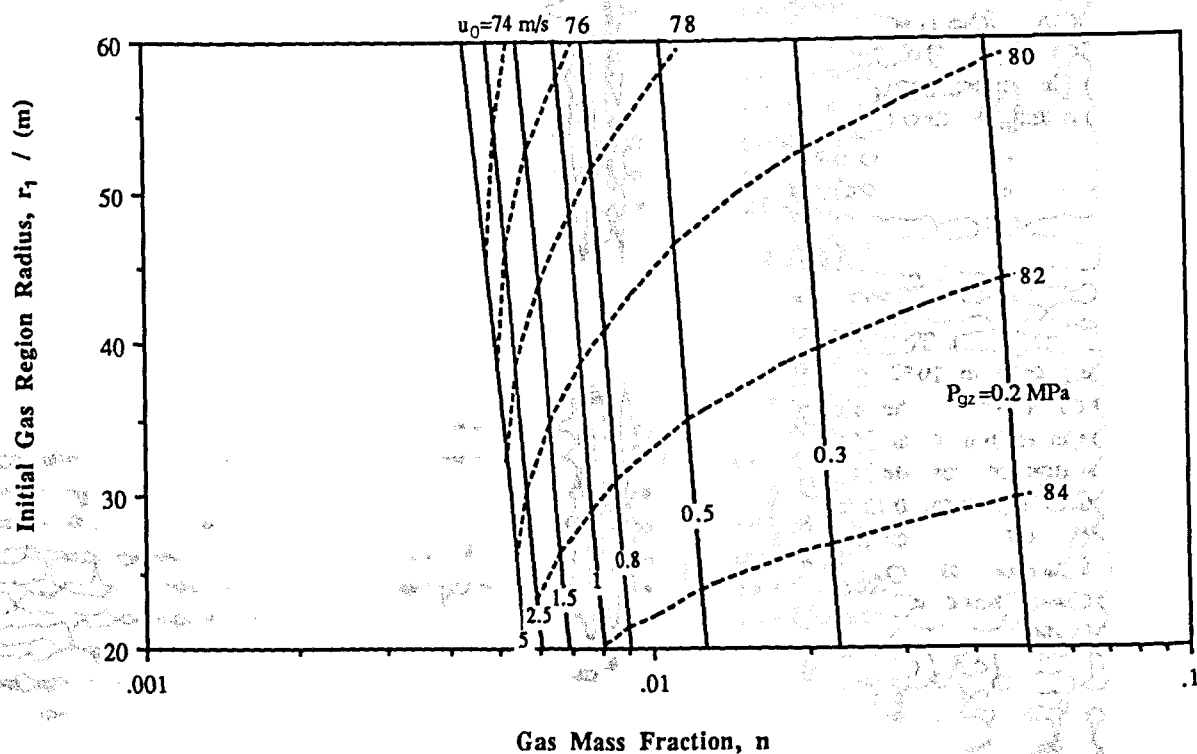


Figure 9. Combinations of r_i , n , P_{gz} and u_0 that project a 2 m diameter block to a distance of 700 m from the centre of the Ukinrek East Maar. Solid curves represent vent pressures of 0.2 to 5 MPa, broken curves represent launch velocities of 74 to 84 m s^{-1} . If a block of 3 m diameter (the largest block found, Self *et al.* 1980) was projected to the same distance, the required launch velocity and gas mass fraction are larger than those shown by less than 2 and 4 per cent, respectively, in the worst cases, and typically less than 1 and 2 per cent respectively.

of the ejected material is thus found to be around 80 to 85 ms⁻¹.

By neglecting air drag entirely, and modelling the trajectories of Type 2 blocks using the vacuum range equation $X = \frac{u^2 \sin 2\phi}{g}$, Self *et al.* (1980) found velocities in the range $u = 80$ to 90 ms⁻¹, the optimum launch angle ($\phi = 45^\circ$) yielding the lowest necessary velocity. This similarity to our values may be attributed to the fact that, as mentioned previously, large blocks (2 m diameter in this case) tend to travel a greater fraction of their vacuum range because their greater masses offer much more inertia against decelerating air drag.

In contrast to our values of 1 to 5 wt per cent, Self *et al.* (1980) estimated that 10 to 30 wt per cent volatiles were required in the exploding mixture using the isothermal treatment of Self *et al.* (1979). This implies large-scale interaction with groundwater and, while it is known that there was a substantial perched aquifer in the glacial till at Ukinrek, it is not clear whether enough of the surface area of the magma body could have interacted with the water to produce such a high weight percentage of gas. We consider this further below.

DISCUSSION

We have shown that it is necessary to take account of the expanding flow field of largely atmospheric gas emanating from a transient explosion source when attempting to estimate the initial velocities of ejected blocks of caprock from their travel distances (Tables 1–6). In all cases, the ranges of blocks ejected into moving gas exceed those of blocks projected into still air (Tables 1–3 of Wilson 1972). The difference in clast range predicted by the two approaches is less marked for large blocks which, due to their greater inertia, are able to travel an appreciable fraction of their vacuum range. However, for projectiles less than about 2 m in diameter, the predicted ranges are much larger using our method and may even exceed the vacuum ranges if the air-clast relative velocity remains sufficiently low over a large distance such that the clasts are partly supported vertically and carried sideways.

We have found, by analysing documented eruptions, that vent pressures, gas concentrations and initial velocities predicted by the current model are usually much smaller than values estimated by previous workers. At Arenal, the projection of a block to a distance of 5 km impacting with a kinetic energy of $\sim 10^{7.6}$ J is possible with vent pressures in the range 5 to 30 MPa, initial velocities in the range 300 to 400 ms⁻¹ and gas mass fractions of ~ 0.04 to 0.1. These values, particularly the pressure given the likely strengths of rocks, seem somewhat more plausible than the values of $P_{gz} = 470$ MPa and $u_0 = 600$ ms⁻¹ that were calculated by Fudali & Melson (1972). At Ngauruhoe, pressures of 1 to 10 MPa, gas mass fractions of 0.02 to 0.06 and velocities of 220 to 250 ms⁻¹ would have sent a 0.8 m projectile to a distance of 2.5 km. For the Ukinrek Maars eruption, the ranges of parameters that will allow a 2 m block to reach a distance of 700 m during the initial crater-forming explosion are $P_{gz} = 0.1$ to 5 MPa, $n = 0.01$ to 0.05, $u_0 = 82$ to 85 ms⁻¹.

One thing apparent from all three of our analyses is that,

while values of the gas/solid fraction are somewhat smaller than values that have been estimated in the past, they are still greater than magmatic volatile contents, which implies a significant concentration of gas in the vent. This, in turn, probably implies some interaction between the magma and meteoric water. This is obviously the case for Ukinrek, where it is known that there is a regional water table at the level of Lake Becharof and a perched aquifer in the overlying glacial till in which the craters were excavated. We would argue that some groundwater interaction is likely in the initiation of most vulcanian eruptions.

We conclude by considering the combinations of circumstances which might lead to the maximum ranges for blocks ejected in transient volcanic explosions. In our model, the size of a block is of no consequence during the stage in which it is accelerated to its maximum velocity, since it is assumed to form part of an effectively continuous shell of material on which acts the pressure of the expanding gas which is giving rise to the explosion. The subsequent range is likely to be large either if the clast is very small, so that it has a negligible terminal velocity in the vertical direction and is effectively carried radially outwards by the expanding atmosphere, or if the clast is very large, in which case it gets very little assistance from the atmosphere near the explosion point in moving radially outwards, but also suffers a negligible amount of drag from the nearly stationary atmospheric gas at great distances from the explosion source. The very small clasts will in any case be distributed in a way determined by the local wind regime; it is the largest clasts which will be most likely to produce recognizable craters that can be used in analysing the eruption. Accordingly, we have calculated ranges for large clasts (up to 5 m diameter). Once a clast size has been selected, the maximum range will occur for a high initial gas pressure, a high gas mass fraction in the explosion source region and a large size of source region.

The initial gas pressure will be limited by the retaining strength of the material overlying the accumulating gas. This may range from a weak glacial till to a dense, coherent rock layer. However, even massive rocks have joints which limit their strength. In volcanic areas, the scenario which represents the greatest strength is where the caprock is a layer of recently emplaced lava or magma intruded at shallow depth. The melt may have invaded cracks in the pre-existing country rocks and will have chilled against them and at any exposed margins. The chilled parts of the magma will have become weak due to the development of cooling cracks, and the uncooled parts of the magma will be weak because they are largely fluid. However, the zones intermediate between these regions will be solid and uncracked, thus having maximal strength. A tensile strength of $\sigma = 20$ MPa is probably an upper limit for such a material (Roberts 1969; Murrell 1969; Tait, Jaupart & Vergnolle 1989). The pressure acting inside a spherical cavity in this material required to cause failure in tension is then $2\sigma = 40$ MPa (Tait *et al.* 1989). The values we have found it necessary to infer above are all significantly smaller than this upper limit, as we would expect.

The amount of gas involved in an explosive event is intimately linked with the geometry of the approach of magma to the surface. The maximum gas mass fraction will occur when exsolved magmatic gas or evaporated meteoric

water accumulates in a space at the top of the column of intruding magma but beneath a rigid carapace. This assertion follows from evaluating the maximum amount of water vapour which can be contained within pores in rocks. The maximum likely porosity of the country rocks adjacent to an intrusion might be about 30 per cent; if this volume fraction of a region is filled with H_2O vapour at the above critical pressure of 40 MPa and a temperature of, say, 500 K, the gas density is 173 kg m^{-3} , making the gas mass fraction about 2.9 per cent. This is somewhat smaller than the values we have inferred from two of our analyses: an inferred mass fraction as high as 10 per cent implies that the volume fraction of the exploding region occupied by gas in more direct contact with magma at a temperature in the range 500 to 1000 K and at 40 MPa pressure lies between about 62 and 76 per cent. The only plausible way to arrange this is to have the gas collect between the juvenile material and a strong overlying layer. Such an arrangement is consistent with the observation that the juvenile rock component in many transient explosions is quite small.

It is difficult to see what factors would determine the largest size of unsupported region that could survive above the gas-filled cavity. This is important because ejected blocks reach their maximum range when the size of the gas cavity is a maximum. For the eruptions studied above, the inference is that this size can range up to $\sim 100 \text{ m}$. Since the launch velocity of ejected blocks is not too strongly dependent on the size of the gas cavity we have taken values up to a factor of 2 larger than this, i.e. 200 m, to be generous. Using the above-mentioned extreme values of block size (5 m), pre-explosion pressure (40 MPa), gas mass fraction (0.1) and pressurised region size (200 m) we have calculated block ranges conservatively by assuming that the explosion site and the impact point are at the same level. We find that ranges up to 11.5 km are possible in these extreme circumstances, more than a factor of two greater than the largest ranges documented in the literature.

CONCLUSIONS

(1) Earlier models of the dispersal of large clasts from transient volcanic explosions have not taken account of the inevitable coupling between the explosion and the surrounding atmosphere, and so have overestimated the atmospheric drag forces on clasts. As a result, they have overestimated the initial gas pressures and gas mass fractions needed to drive these explosions.

(2) Transient vulcanian explosions appear typically to require initial gas pressures significantly less than 40 MPa, consistent with the strengths of the rocks under which pressure accumulation occurs. Inferred gas mass fractions of 0.01 to 0.1 (1 to 10 per cent) imply that some meteoric water, in addition to magmatic volatiles, is commonly involved. Launch velocities of large clasts span values from a few tens of m s^{-1} to $\sim 400 \text{ m s}^{-1}$.

(3) If extreme combinations of the most favourable values of controlling parameters (gas pressure, gas fraction,

and size of explosion source) are taken, it is predicted that large ($>3 \text{ m}$ diameter) clasts could possibly be ejected to ranges up to about 12 km, more than twice as far as in any eruption of this kind yet documented.

ACKNOWLEDGMENTS

SAF thanks the Science and Engineering Research Council for a research studentship. We are also grateful to J. Gilbert and an anonymous reviewer for valuable comments and suggestions.

REFERENCES

- Basaltic Volcanism Study Project, 1981. *Basaltic Volcanism on the Terrestrial Planets*, Pergamon Press, Inc., New York.
- Fudali, R. F. & Melson, W. G., 1972. Ejecta velocities, magma chamber pressure and kinetic energy associated with the 1968 eruption of Arenal Volcano, *Bull. Volc.*, **35**, 383–401.
- Kienle, J., Kyle, P. R., Self, S., Motyka, R. J. & Lorenz, V., 1980. Ukinrek Maars, Alaska, I. April 1977 eruption sequence, petrology and tectonic setting, *J. Volc. Geotherm. Res.*, **7**, 11–37.
- McBirney, A. R., 1973. Factors governing the intensity of explosive andesitic eruptions, *Bull. Volc.*, **37**, 443–453.
- Melson, W. G. (ed.), 1972. *Arenal Volcano, Costa Rica: Catastrophic eruption of 1966–70 and pre-eruption history*, Smithsonian Contributions to the Earth Sciences, Smithsonian Institution Press, Washington DC.
- Melson, W. G. & Saenz, R., 1973. Volume, energy and cyclicity of eruptions of Arenal Volcano, Costa Rica, *Bull. Volc.*, **10**, 59–87.
- Murrell, S. A. F., 1969. Global tectonics, rock mechanics and the mechanism of volcanic intrusions, in *Mechanisms of Igneous Intrusion*, pp. 231–244, eds Newall, G. & Rast, N., Gallery Press, Liverpool.
- Nairn, I. A., 1976. Atmospheric shock waves and condensation clouds from Ngauruhoe explosive eruptions, *Nature*, **259**, 190–192.
- Nairn, I. A. & Self, S., 1978. Explosive eruptions and pyroclastic avalanches from Ngauruhoe in February 1975, *J. Volc. Geotherm. Res.*, **3**, 39–60.
- Roberts, J. L., 1969. The intrusion of magma into brittle rocks, in *Mechanisms of Igneous Intrusion*, pp. 287–362, eds Newall, G. & Rast, N., Gallery Press, Liverpool.
- Self, S., Wilson, L. & Nairn, I. A., 1979. Vulcanian eruption mechanisms, *Nature*, **277**, 440–443.
- Self, S., Kienle, J. & Huot, J.-P., 1980. Ukinrek Maars, Alaska, II. Deposits and formation of the 1977 craters, *J. Volc. Geotherm. Res.*, **7**, 39–65.
- Steinberg, G. S., 1977. On the determination of the energy and depth of volcanic explosions, *Bull. Volc.*, **40**, 1–5.
- Tait, S. R., Jaupart, C. & Vergnolle, S., 1989. Pressure, gas content and eruptive periodicity of a shallow crystallising magma chamber, *Earth planet Sci. Lett.*, **92**, 107–123.
- Wilson, L., 1972. Explosive volcanic eruptions—II. The atmospheric trajectories of pyroclasts, *Geophys. J. R. astr. Soc.*, **30**, 381–392.
- Wilson, L., 1980. Relationships between pressure, volatile content and ejecta velocity in three types of volcanic explosion, *J. Volc. Geotherm. Res.*, **8**, 297–313.